

# Molecular Bands in the Spectra of M Stars

Ya. V. Pavlenko\*

*Main Astronomical Observatory, National Academy of Sciences of Ukraine,  
ul. Akademika Zabolotnoho 27, Kiev, 03680 Ukraine*

Received February 25, 2014; in final form, March 17, 2014

**Abstract**—The profiles of the main molecular bands in the spectral-energy distributions (SEDs) of M stars have been calculated. The calculations of the individual band profiles were performed using the just-overlapping-lines approximation. Information about the oscillator strengths and the sources of the spectroscopic data for specific transitions between electronic levels of molecules is provided. The calculations of theoretical SEDs for M stars were performed using available lists of molecular lines for sources of bound–bound opacity in the atmospheres of oxygen–sequence stars. The observed SEDs of the oxygen–sequence red giant HD 148783 (30 Her) and the M dwarf 2MASS J22424129–2659272 are reproduced. The dependence of the calculated SEDs of the M giant on the adopted metallicity and carbon abundance is studied. The observed SEDs of HD 148783 and 2MASS J22424129–2659272 are described well by theoretical spectra calculated for model atmospheres with  $T_{\text{eff}}/\log g/[\text{Fe}/\text{H}] = 3250/-0.4/0$  and  $3000/5.0/0$ , respectively.

**DOI:** 10.1134/S1063772914110043

## 1. INTRODUCTION

Late-type stars are most numerous among the population of our Galaxy. Low-mass dwarf stars comprise >70% of the total number of stars of the Galaxy [1], and dwarf stars of spectral types M, L, T clearly dominate in terms of their numbers among the other populations of the Galaxy. Although their total mass, according to various estimates, makes up 5–15% of the total mass of the Galaxy, dwarf stars also constitute an important component of dark mass in the form of baryonic matter. These estimates are very likely also applicable for other galaxies. The study of stars with masses below  $0.6 M_{\odot}$  is an important task of modern astrophysics. The population of late-type dwarfs includes brown dwarfs—substellar objects with masses below  $0.075 M_{\odot}$  [2] that occupy an intermediate position between stars and giant planets. TiO absorption bands, characteristic of M stars, are observed in the spectra of most of these low-mass dwarfs at least at the early stages of their evolution.

At the same time, M giants are not as numerous. They are of interest for our understanding of the nature of late-type stars more massive than M dwarfs. Note that M giants have high luminosities ( $2.2 < L_{\text{bol}} < -2.2$ ), and so are accessible to observation at greater distances than dwarfs. Therefore, analyses of the spectra of M giants at different distances from

the centre of the Galaxy and in its bulge can reveal information about the chemical evolution of different parts of the Galaxy [3].

The spectra of M stars are formed in the presence of very low temperatures and, in the case of ultra-cool dwarfs, high pressures. This introduces additional difficulties for developing and applying techniques for interpreting them. The maximum energy radiated by these stars is in the infrared. At the same time, their optical spectra are of special interest for many studies. For example, the realization of the so-called “lithium test” [4] requires analyses of lines of neutral lithium in the optical spectra of M dwarfs. Absorption lines of potassium and sodium are also found here, and can be used for quantitative analyses of the physical conditions in the stellar atmospheres. All these absorption lines demonstrate strong dependences on the temperature and gravity [5]. In M-dwarf spectra, they form against the background of strong molecular bands, with systems of TiO bands dominating in terms of their intensity [6]. Strictly speaking, the spectral classification of M stars is based on variations in the intensity of these bands, namely, their enhancement in the transition from early M to late M stars. When the effective temperatures of dwarfs decrease below 2400 K, the depletion of molecules in their atmospheres due to the binding of atoms of Ti, V, and other metals in dust particles [7] becomes appreciable. As a consequence, the shape of the SEDs of cool dwarf stars in the optical changes fundamentally [8]. This

\*E-mail: yp@mao.kiev.ua

**Table 1.** Positions of the  $(v'', v') = (0, 0)$  band heads of the TiO molecule and their oscillator strengths  $f_{el}$ 

System	Transition	Position of the (0,0) band head, Å	$f_{el}$		
			[24]	[12]	[25]
$\alpha$	$C^3\Delta - X^3\Delta$	5170.7	0.105	0.1288	0.106
$\beta$	$c^1\Phi - a^1\Delta$	5605.2	0.176	0.1621	0.1250
$\gamma'$	$B^3\Pi - X^3\Delta$	6192.5	0.108	0.1514	0.0935
$\gamma$	$A^3\Phi - X^3\Delta$	7095.8	0.092	0.1193	0.0786
$\delta$	$b^1\Pi - a^1\Delta$	8407.6	0.048	0.0581	0.0480
$\epsilon$	$E^3\Pi - X^3\Delta$	8870.9	0.032	0.0025	0.0023
$\phi$	$b^1\Pi - a^1\Delta$	11044.0	0.052	0.0668	0.0178

**Table 2.** Positions of the band heads of other molecules and their oscillator strengths  $f_{el}$ 

System	Transition	Position of the (0,0) band head, Å	$f_{el}$	Reference
AlO	$B^2\Sigma^+ - X^2\Sigma^+$	4845	0.039	[19]
CrH	$A^6\Sigma^+ - X^6\Sigma^+$	8620	0.001	[26]
VO	$B^4\Pi^+ - X^4\Sigma^+$	7930	0.120	[24]
FeH	$F^4\Delta_i - X^4\Delta_i$	8694	—	[27]
CaH	$B^2\Sigma^+ - X^2\Sigma^+$	6900	0.050	—
MgH	$A^2\Pi_r - X^2\Sigma^+$	5208	0.059	[19]
CN(blue)	$B^2\Sigma^+ - X^2\Sigma^+$	3884	0.036	[19]

formed the basis for introducing the new spectral type L for stars cooler than M dwarfs [9, 10].

Recently, techniques for determining the effective temperatures of M dwarfs and M giants by fitting their observed optical spectra have been developed. A series of spectral indices has been proposed, which are in most cases ratios of fluxes formed in the heads and tails of the TiO bands [11].

Some progress in studies of the spectra of M stars has been achieved in recent years due to the appearance of high-resolution spectral observations of M stars and substantial improvement of our knowledge

of the sources of opacity determining their optical and infrared spectra, including the availability of lists of TiO absorption lines calculated in various studies [12, 13], which yield similar results when used.

We adopted the following structure for this paper. Section 2 describes the technique used in our calculations of the profiles of individual bands of TiO molecule and other molecules that can form features in the absorption spectrum of M stars. The input parameters used in the calculations are given. The calculated molecular-band profiles are shown in Section 2.1. Sections 3.1 and 3.2 give reproductions of the observed SEDs of the M giant HD 148783 and the M dwarf 2MASS J22424129–2659272; our results for the effective temperatures of these stars are also given. Our results are discussed in Section 4.

## 2. PROCEDURE USED FOR THE CALCULATIONS

In this study, we have essentially calculated the SEDs of stars. However, for simplicity, we will use the term synthetic spectrum in place of SED. In our synthetic-spectrum calculations for M dwarfs and M giants, we used model atmospheres from the NEXTGEN grid [14] and calculated with the SAMI2 code [15], respectively. The synthetic spectra were calculated applying classical approximations with the WITA618 software [16]. We used the same system of continuum opacity sources [5] as in the calculation of the model atmospheres. All the calculations were carried out for the solar composition, taken from [17].

### 2.1. Profiles of Molecular Bands

One problem explored in our study was the calculation of individual systems of bands of diatomic molecules that contribute to the optical spectra of M stars. We calculated the molecular line profiles using the technique described by Nersisyan et al. [18] for this purpose. To simplify the presentation of this material, we used the Just Overlapping Line Approximation (JOLA). We optimized the algorithm and codes of the BIGF1 software to reduce the calculation time. The modified subroutine was included in the WITA software [6].

The JOLA technique enabled us to calculate the profiles of molecular bands separately. Naturally, the fine structure of the molecular bands is not taken into account in this case, but their separation into the P, Q, and R branches is. The data for the molecular terms and the transitions between them were taken from various sources [19–21]. The profiles of strong molecular bands calculated using JOLA and using detailed line lists mutually consistent [22], and, as a whole, describe the observed spectra satisfactorily.

Of course, such a comparison is meaningful only for the case of observed spectra with moderate and low dispersion, when the rotational structure of the molecular spectra is no longer exhibited due to the blurring of separate absorption lines as a consequence of instrumental broadening, appreciable macroturbulence velocities in the atmosphere, or fairly rapid rotation of the star itself.

The most problematic aspect of such calculations is the choice of the system of oscillator strengths for the corresponding electronic transitions. Adopted values of  $f_{el}$  differ by up to 30%, even for systems of fairly well studied molecules that have been known for a relatively long time [23–25]. We used for the TiO absorption bands the system of oscillator strengths of Alvarez and Plez [23], adopted by Plez [12] for the calculation of detailed lists of lines of this molecule. Table 1 presents a list of TiO molecular bands for which we calculated absorption profiles, and the sources of spectroscopic data for each. The sources of the spectroscopic data for the other molecules taken into account are given in Table 2.

The results of the calculations for the main systems of bands of TiO and other molecules forming the SEDs of M stars are shown in Figs. 1 and 2. These calculations were carried out for the M-dwarf model atmosphere from the grid of Hauschildt et al. [28] with  $T_{\text{eff}}/\log g/[\text{Fe}/\text{H}] = 2800/5.0/0$ . This model atmosphere corresponds to spectral type M6V.

Owing to the absence of corresponding spectroscopic constants for FeH and H<sub>2</sub>O in our list of JOLA opacity sources, the profiles of their bands were calculated using the line lists of Dulick et al. [27] and Barber et al. [29], respectively.

There is no single system of bands of any single molecule that dominate over a broad wavelength interval in the optical spectra of M stars, as in the case of C stars [30]. Some bands are obviously stronger than others in relatively narrow spectral ranges; these belong to TiO (the  $\gamma$ ,  $\gamma'$ ,  $\epsilon$  system of bands), as well as other molecules (MgH, CaH, CrH, FeH).

The profiles of the bands presented in Figs. 1 and 2 are accessible on the web in the form of graphs and ASCII-files ([www.mao.kiev.ua/staff/yp/Results/M-stars/mb.htm](http://www.mao.kiev.ua/staff/yp/Results/M-stars/mb.htm)); these can be used to identify absorption features in the spectra of late-type stars.

## 2.2. Synthetic Spectra

The synthetic spectra we used to reproduce the observed optical SEDs of particular stars were calculated in the “line after line” approximation, including absorption lines taken from various lists:

- the VALD list of atomic lines [31],
- TiO lines calculated by Plez [12],
- the list of CN and MgH lines from CD-ROM no. 18 Kurucz [32],
- the lists of CrH and FeH lines calculated by Burrows et al. [33] and Dulick et al. [27], and
- the list of H<sub>2</sub>O absorption lines calculated by Barber et al. [29].

For molecules such as VO and CaH, no line lists are openly available yet; the opacities in bands of these molecules were calculated in the JOLA approximation in our synthetic-spectrum calculations.

The profiles of absorption lines were determined assuming a Voigt function, with the damping constants determined in the approximation of Unsöld [34]. The microturbulent velocity was assumed to be constant and equal to  $V_t = 2$  km/s across the depth of the atmosphere.

## 3. FITS TO THE M-STAR's SEDs

To get an idea of our ability of reproducing the observed spectra of M stars using synthetic spectra calculated for modern model atmospheres and line lists, we carried out SED calculations for two stars—HD 148783 and the M dwarf 2MASS J22424129–2659272. Their effective temperatures are similar (3250 and 3000 K, respectively), but their luminosities differ considerably.

### 3.1. The Spectrum of HD 148783

The red giant HD 148783 (also known as V\*g Her, AG+411390, BD+422714, FK5 3303, GSC 03066–02214, 30 Her, HIC 80704, HIP 80704, HR 6146, IRAS 16269+4159) has been included in a number of photometric and spectroscopic studies. Its metallicity is believed not to differ strongly from the solar value. This star has been used as a standard in tests of techniques for determining the main parameters of stars using spectroscopic methods [35] and in studies of changes in the chemical compositions of stars in the red-giant stage [36]. Assuming the solar metallicity, the atmospheric effective temperature  $T_{\text{eff}}$  and gravity  $\log g$  of this red giant have been estimated to be  $3250 \pm 100$  K and  $0.2 \pm 0.3$  [35–37]. These atmospheric parameters for HD 148783 were obtained by analyzing high-dispersion spectra using model atmospheres; i.e., by analyzing the equivalent widths and absorption profiles of atomic and ionic lines in the infrared.

We successfully reproduced the SED of HD 148783. The observed spectrum of this giant was taken from the STELIB database [38]. We essentially

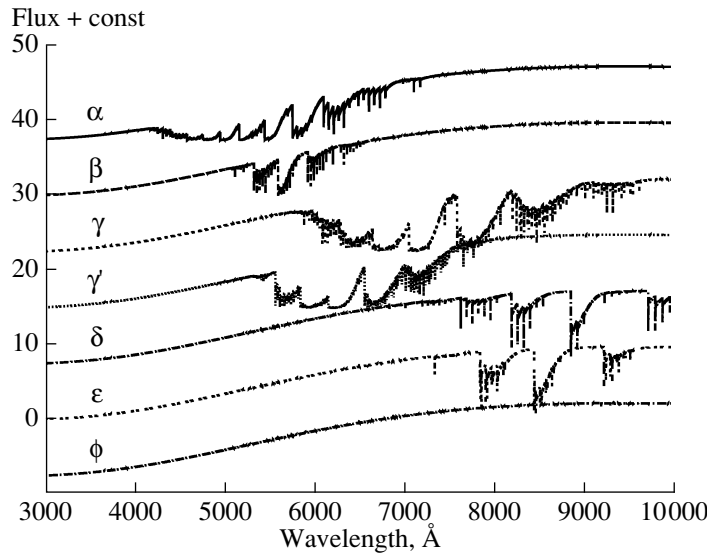


**Fig. 1.** Profiles of systems of bands of TiO alone in the optical and near-infrared spectra of M stars calculated with the oscillator strengths from [23] (Table 1).

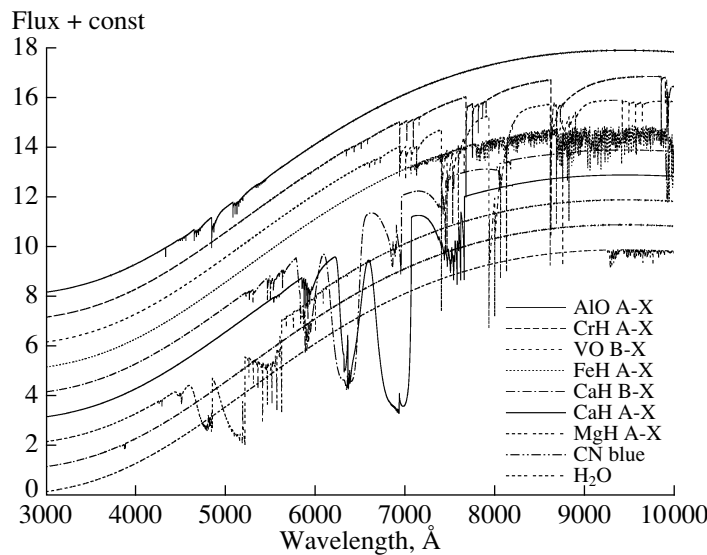


**Fig. 2.** Profiles of systems of bands of diatomic molecules in the optical spectrum of M stars calculated with the oscillator strengths listed in Table 2.

independently determined the effective temperature through our fit to the observed SED of HD 148783.

The atmospheric gravity of this red giant is known fairly poorly, as is common for most stars of this spectral type. To study the effect of  $\log g$  on our results, we calculated a grid of models using the SAM12 software [15]. Model atmospheres assuming the solar metallicity were calculated for a fairly broad interval of effective temperatures  $T_{\text{eff}} = 3050\text{--}3450$  K in steps of 100 K and for gravities  $\log g = -0.3 \dots 0.5$  in steps of 0.2.

The synthetic spectra were calculated using tech-

nique and line lists indicated in Section 2. We compared the theoretical and observed spectra employing the procedure used in [39, 40].

We took into account the broadening of the observed spectra due to the presence of macroturbulent motions in the atmosphere of the red giant and instrumental broadening. The synthetic spectra were convolved with a Gaussian corresponding to the total (instrumental + macroturbulence) spectral resolution  $R = 15\,000$ ; further, they were compared with the observed SED of HD 148783. The best fit was found by determining the minimum sum of the differences

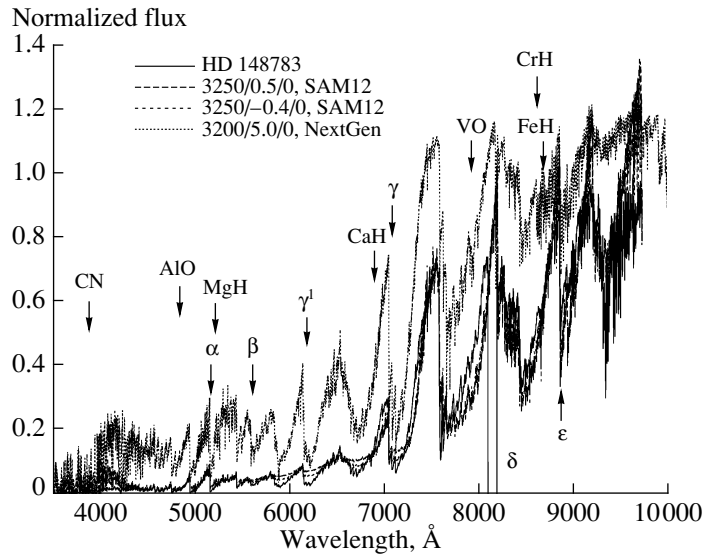


**Fig. 3.** Comparison of the SED of the red giant HD 148783 with those calculated for the SAM12 model atmospheres with  $T_{\text{eff}} = 3250$  K,  $\log g = 0.5$  and  $-0.4$ . For comparison, the theoretical SED of an M dwarf with  $T_{\text{eff}} = 3200$  K and  $\log g = 5.0$  is shown.

between the observed and calculated fluxes,

$$S(f_h^*) = \sum_{\nu} (F_{\nu} - f_h F_{\nu}^x)^2,$$

where  $F_{\nu}$  and  $F_{\nu}^x$  are the observed and calculated fluxes, respectively, and  $f_h$  is a normalization parameter.

The comparison of the observed and calculated SEDs was carried out at wavelengths 4400–8090 Å, except for the narrow spectral range 8165–8220 Å, where no emission is observed in the observed spectrum (Fig. 3).

At wavelengths shorter than 4400 Å, the difference between the calculated and observed spectra becomes appreciable: the observed fluxes become lower than can reasonably be interpreted as an effect of incompleteness of the list of opacity sources used in our calculations. This “opacity deficit” in the short-wavelength part of the spectrum has a long history [41], and a full discussion is beyond the scope of this paper. We note, however, that eliminating wavelengths  $\lambda < 4400$  Å from our analysis has virtually no effect on our results.

The quality of the reproduction of the observed SED is higher for the lower the minimization parameter  $S$ . The parameter  $S$  displays an appreciable dependence on the adopted effective temperature  $T_{\text{eff}}$  for the model atmosphere and, to some extent, on the gravity  $\log g$  (Fig. 4). The minimum of  $S$  occurs for  $T_{\text{eff}} = 3250$  K, consistent with other estimates of the effective temperature.

To illustrate our procedure, we chose a red giant whose iron abundance is not very different from the solar value. However, the metallicity of the observed stars is not always known. At the same time, this parameter has great importance in calculations of the TiO-band intensities, which ultimately determine the shape of the SED in the optical spectrum of an M star. We carried out additional studies to investigate the influence of the adopted metallicity on the quality of the fit to the observed spectrum. We calculated a grid of model atmospheres with  $T_{\text{eff}} = 3250$  K,  $\log g = -0.4$ , and metallicities  $[\text{Fe}/\text{H}] = -1.0, -0.5, -0.2, 0.0, 0.2, 0.5$ , and  $1.0$ , and then calculated theoretical SEDs for these model atmospheres, which we compared to the observed fluxes of HD 148783. We used the procedure described above, based on minimizing  $S$ . The resulting values of  $S$  for all these calculated SEDs are shown in Fig. 5. The minimum of  $S$  occurs at  $[\text{Fe}/\text{H}] = -0.1 \pm 0.1$ , in reasonably good agreement with the most recent determinations of the metallicity of this star [35, 37].

We do not give the best agreement of the calculated SEDs with  $[\text{Fe}/\text{H}] = -0.1$  and the observed SEDs, because this figure is virtually identical to Fig. 3, both in overall and particulars.

We indicate the fairly broad range of metallicities determined by our procedure, since another important parameter, namely, the atmospheric carbon abundance of HD 148783, can also influence our solution. A substantial fraction of the oxygen and carbon atoms in cool atmospheres are bound in CO molecules.

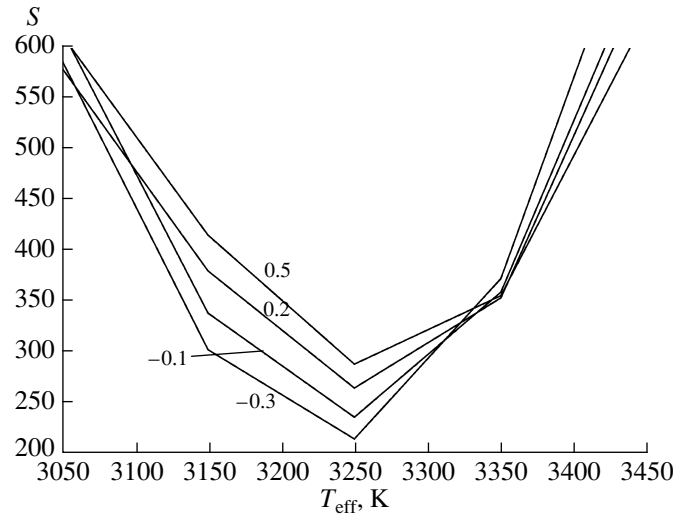


**Fig. 4.** Minimization parameter  $S$  calculated in our reproduction of the observed spectrum of HD 148783 using theoretical spectra for model atmospheres with various  $T_{\text{eff}}$  and  $\log g$  values. The  $\log g$  values are indicated by the corresponding curves.

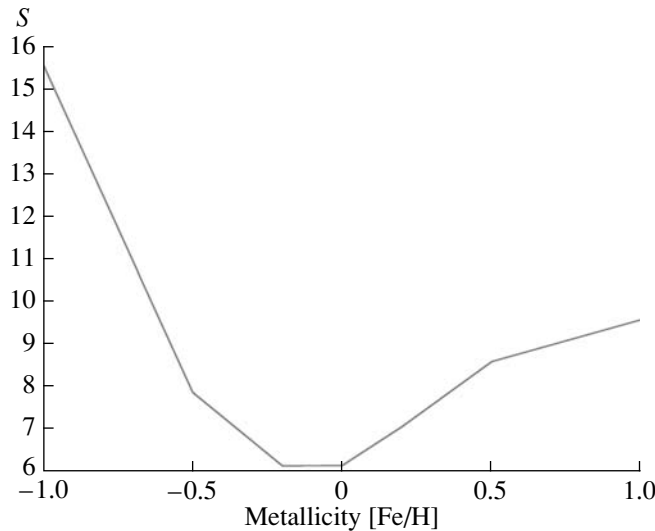


**Fig. 5.** Same as Fig. 4 for model atmospheres with different metallicities. For all the models,  $T_{\text{eff}} = 3250$  K and  $\log g = -0.4$ .

Nevertheless, a change in the atmospheric carbon abundance of the red giant affects the number of oxygen atoms that can form TiO molecules. The change in the atmospheric carbon abundance after the star's outgoing from the main sequence is fully explained by natural processes [42]. Formally, a reduction of carbon in the stellar atmosphere could be manifest as an increase in its metallicity, since the number of TiO, VO, and H<sub>2</sub>O molecules grows in this case. In many respects, absorption by these molecules determines the blanketing effect in the atmospheres of M stars [15], which affects their SEDs.

We studied this effect by comparing the observed fluxes for HD 148783 with the SEDs calculated for model atmospheres with  $T_{\text{eff}} = 3250$  K,  $\log g = -0.4$ , and  $[\text{Fe}/\text{H}] = 0$ , but with different carbon abundances  $\log N(\text{C}) = -4.49, -4.29, -3.99, -3.69, -3.39, -3.29$ , and  $-3.19$ . The changes in the spectra due to changes in the carbon abundance are ultimately reflected in the dependence of  $S$  on  $\log N(\text{C})$  (Fig. 6). In this case, the model atmospheres and the SEDs were calculated for the specified carbon abundances; i.e., the total effect of the modified

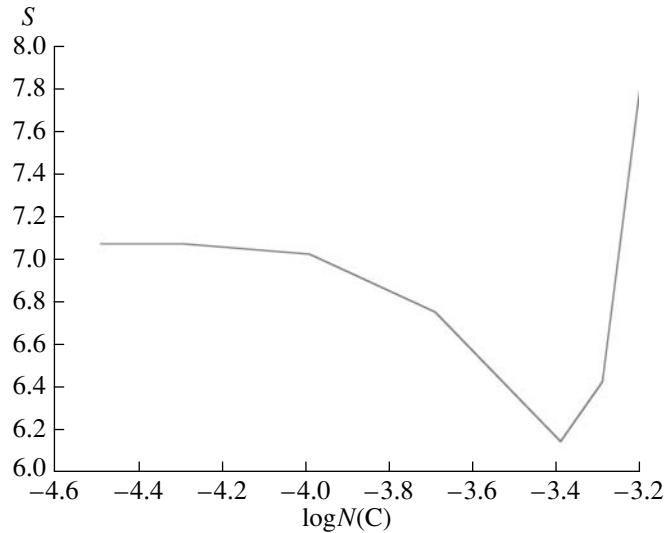


**Fig. 6.** Same as Fig. 4 for model atmospheres with various  $\log N(\text{C})$  values. For all the models,  $T_{\text{eff}} = 3250$  K and  $\log g = -0.4$ . The abundances of other elements are solar.

structure of the atmospheric model and changes in the dissociative equilibrium is exhibited.

The minimum of  $S$  in Fig. 5 is near  $\log N(\text{C}) = -3.39$ , which corresponds to the solar carbon abundance [43]. Naturally, a more accurate estimate of the atmospheric carbon abundance of HD 148783 requires other, more refined techniques, based, e.g., on the analysis of CO-band intensities in the infrared [39].

### 3.2. The Spectrum of 2MASS J22424129–2659272

We also modelled the observed SED of a dwarf M star from the sample of spectra analyzed in [44] as part of a study of stars with similar proper motions in the solar neighborhood. The observations of this dwarf were conducted on the UVES spectrograph of the ESO-VLT-U2 telescope; details of the reduction are given in [45, 46]. As a whole, the data were obtained with high spectral resolution ( $R = 70\,000$ ), but with fairly low signal-to-noise ratio (about 20, decreasing appreciably in the short-wavelength part of the spectrum). Nevertheless, important features such as the resonance lines of potassium at  $7800 \text{ \AA}$  and the subordinate line of sodium at  $8200 \text{ \AA}$ , which are crucial for the analysis of spectra of late-type dwarfs, are detected fairly confidently.

The calculations of the theoretical spectra were performed using the same procedure and input data as for the red giant (Section 3.1). Model atmospheres from the grid of Hauschildt et al. [28] were used. Synthetic spectra were calculated for models with  $T_{\text{eff}} = 2800\text{--}3400$  K and  $\log g = 5.0$ . This gravity was

chosen because the corresponding calculated spectra described the profiles of the strong resonance lines of potassium at  $7800 \text{ \AA}$  and the subordinate triplet at  $8200 \text{ \AA}$  (Fig. 7) better than those for other gravities.

The calculated synthetic spectra were compared with the observed spectra. Here too, the parameter  $S$  explicitly depends on the specified effective temperature of the model atmosphere, and the minimum of  $S$  is clearly located at  $T_{\text{eff}} = 3000 \pm 50$  K (Fig. 8).

## 4. DISCUSSION

We have calculated the profiles of individual molecular bands shown in Figs. 1 and 2 using a simple technique. This was done in order to show their main characteristics, such as the positions of the band heads and the decrease in the intensities to either side of the bands. These calculations also give us an idea of the relative intensities of individual bands. The data obtained can be used in qualitative and quantitative analyses of the spectra of M stars.

Note that the synthetic spectra we used for our analysis of the SEDs of particular M stars were calculated with a more modern approach to treating molecular absorption, using detailed lists of atomic and molecular lines. However, the JOLA procedure was still used when calculating the opacity in systems of individual molecular bands for which reliable line lists are not available [47].

Our results were obtained in the framework of classical approximations. The model atmospheres we used were calculated with a set of opacity sources that was as complete as possible, in a wavelength interval

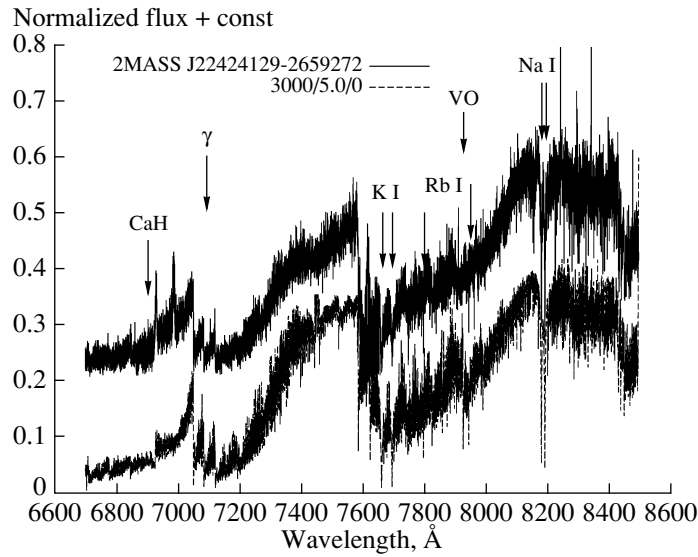


**Fig. 7.** Comparison of the observed SED of 2MASS J22424129–2659272 and the calculated SED for the NextGen model atmosphere with  $T_{\text{eff}} = 3000$  K,  $\log g = 5.0$ , and  $[\text{Fe}/\text{H}] = 0$ . The observed and calculated fluxes are shifted by a constant amount for clearer viewing of the results. The positions of the (0,0) band heads for the  $\gamma$  system of TiO and the  $\text{B}^4\Pi^+X^4\Sigma^+$  system of VO are shown together with the positions of strong atomic lines in the spectrum of 2MASS J22424129–2659272.

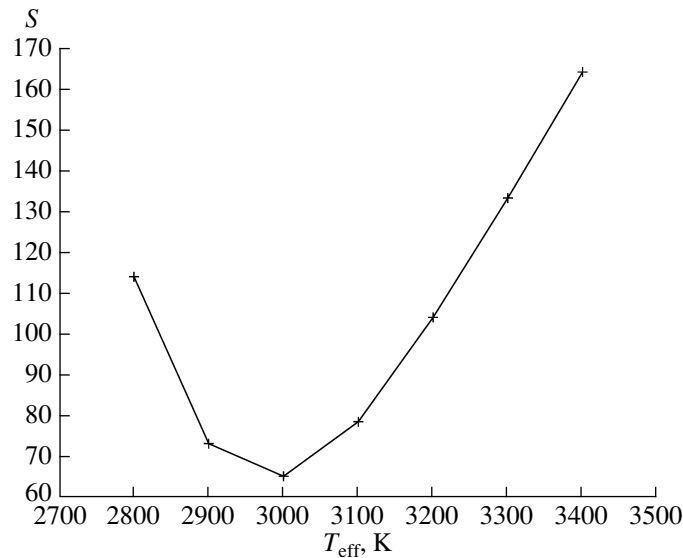


**Fig. 8.** Minimization parameter  $S$  for the fit of the observed spectrum of 2MASS J22424129–2659272 with the theoretical spectra for model atmospheres with various  $T_{\text{eff}}$  and with  $\log g = 5.0$ .

that was as broad as possible. Note here that the calculated SED of an M star also depends on the metallicity in its atmosphere. In our case, we chose stars with known metallicity for our analysis, which enabled us to minimize the influence of this factor on the results.

Owing to the difference in the dissociative equilibrium in the atmospheres of M dwarfs and M giants with the same effective temperature, the intensities of the main bands determining the shape of SED in optical spectrum are considerably different.



The best reproduction using the calculated spectra was obtained for effective temperatures that are fairly consistent with earlier estimates, in spite of the fact that our values were obtained using a different technique. Therefore, we conclude that our technique can be used to address numerous problems involving finding the main characteristics of M stars, both giants and dwarfs (see [48, 49]).

### ACKNOWLEDGMENTS

This work was supported by the FP7 POSTAG-BinGALAXIES International Research Staff Exchange Scheme (grant no. 269193). This research has used the SIMBAD, VALD, and ADS databases. Special thanks are due to the authors of the STELIB database J.R.A. Clark and M.C. Gálvez-Ortiz for the spectra of 2MASS J22424129–2659272 and to L.A. Yakovina for useful advice. We thank the anonymous referee for helpful comments.

### REFERENCES

1. J. J. Bochanski, S. L. Hawley, K. R. Covey, A. A. West, I. N. Reid, D. A. Golimowski, and Z. Ivezić, *Astron. J.* **139**, 2679 (2010).
2. R. Rebolo, E. L. Martin, G. Basri, G. W. Marcy, and M. R. Zapatero Osorio, *Astrophys. J. Lett.* **469**, L53 (1996).
3. J. A. Frogel and A. W. Whitford, *Astrophys. J.* **320**, 199 (1987).
4. R. Rebolo, E. L. Martin, and A. Magazzu, *Astrophys. J. Lett.* **389**, L83 (1992).
5. Ya. Pavlenko, M. R. Zapatero Osorio, and R. Rebolo, *Astron. Astrophys.* **355**, 245 (2000).
6. Ya. V. Pavlenko, R. Rebolo, E. L. Martin, and R. J. Garcia Lopez, *Astron. Astrophys.* **303**, 807 (1995).
7. Ya. V. Pavlenko, *Astron. Rep.* **42**, 787 (1998).
8. Ya. V. Pavlenko, *Odessa Astron. Publ.* **10**, 76 (1997).
9. E. L. Martin, X. Delfosse, G. Basri, B. Goldman, T. Forveille, and M. R. Zapatero Osorio, *Astron. J.* **118**, 1005 (1999).
10. J. D. Kirkpatrick, I. N. Reid, J. Liebert, R. M. Cutri, B. Nelson, Ch. A. Beichman, C. C. Dahn, D. G. Monet, J. E. Gizis, and M. F. Skrutskie, *Astrophys. J.* **519**, 802 (1999).
11. G. Worthey, S. M. Faber, J. J. Gonzalez, and D. Burstein, *Astrophys. J. Suppl. Ser.* **94**, 687 (1994).
12. B. Plez, *Astron. Astrophys.* **337**, 495 (1998).
13. D. Schwenke, in *Proceedings of the Faraday Discussions No. 109 on Chemistry and Physics of Molecules and Grains in Space*, Ed. by P. J. Sarre (Faraday Division, R. Soc. of Chemistry, London, 1998), p. 321.
14. P. Hauschildt and F. Allard, *Astrophys. J.* **512**, 377 (1999).
15. Ya. V. Pavlenko, *Astron. Rep.* **47**, 59 (2003).
16. Ya. V. Pavlenko, *Astrophys. Space Sci.* **253**, 43 (1997).
17. E. Anders and N. Grevesse, *Geochim. Cosmochim. Acta* **53**, 197 (1989).
18. S. E. Nersisyan, A. V. Shavrina, and A. A. Yaremchuk, *Astrofizika* **30**, 147 (1989).
19. L. A. Kuznetsova, N. E. Kuz'menko, Yu. Ya. Kuzyakov, and Yu. A. Plastinin, *Probabilities of Optical Transitions in Diatomic Molecules* (Nauka, Moscow, 1980) [in Russian].
20. K. P. Huber and G. Herzberg, *Constants of Diatomic Molecules* (Van Nostrand Reinolds, New York, 1979), p. 716.
21. N. E. Kuz'menko, L. A. Kuznetsova, and Yu. A. Kuzyakov, *Frank–Condon Factors of Diatomic Molecules* (Mosk. Gos. Univ., Moscow, 1980) [in Russian].
22. Ya. V. Pavlenko, *Astron. Rep.* **44**, 219 (2000).
23. R. Alvarez and B. Plez, *Astron. Astrophys.* **330**, 1109 (1998).
24. F. Allard, P. Hauschildt, and D. Schwenke, *Astrophys. J.* **540**, 1005 (2000).
25. N. V. Dobrodey, *Astron. Astrophys.* **365**, 642 (2001).
26. Ya. V. Pavlenko, *Astron. Rep.* **43**, 748 (1999).
27. M. Dulick, C. W. Bauschlincher, and A. Burrows, *Astrophys. J.* **594**, 651 (2003).
28. P. H. Hauschildt, F. Allard, and E. Baron, *Astrophys. J.* **512**, 377 (1999).
29. R. J. Barber, J. Tennyson, G. J. Harris, and R. Tolchenov, *Mon. Not. R. Astron. Soc.* **368**, 1087 (2006).
30. L. A. Yakovina, A. F. Pugach, and Ya. V. Pavlenko, *Astron. Rep.* **53**, 187 (2009).
31. F. Kupka, N. Piskunov, T. A. Ryabchikova, H. C. Stempels, and W. W. Weiss, *Astron. Astrophys. Suppl. Ser.* **138**, 119 (1999).
32. R. L. Kurucz, *CD-ROM, Nos. 1–23* (Smithsonian Astrophys. Observ., Cambridge, MA, 1993).
33. A. Burrows, S. R. Ram, P. Bernath, C. M. Sharp, and J. A. Milsom, *Astrophys. J.* **577**, 986 (2002).
34. A. Unsold, *Physik der Sternatmosphären*, 2nd ed. (Springer, Berlin, 1955).
35. J. S. Carr, K. Selgryn, and S. G. Balachandra, *Astrophys. J.* **530**, 307 (2000).
36. V. V. Smith and D. L. Lambert, *Astrophys. J.* **294**, 326 (1995).
37. S. V. Ramirez, K. Selgryn, J. S. Carr, S. C. Balachandran, R. Blum, D. M. Tendrup, and A. Steed, *Astrophys. J.* **535**, 205 (2000).
38. J.-F. Le Borgne, G. Bruzual, R. Pello, A. Lancon, B. Rocca-Volmerange, B. Sanahuja, D. Schaerer, C. Soubiran, and R. Vilchez-Gomez, *Astron. Astrophys.* **402**, 433L (2003).
39. Ya. V. Pavlenko and H. R. A. Jones, *Astron. Astrophys.* **397**, 967 (2002).
40. Ya. V. Pavlenko, Ch. E. Woodward, M. T. Rushton, B. Kaminsky, and A. Evans, *Mon. Not. R. Astron. Soc.* **404**, 216 (2010).
41. C. Allende Prieto, I. Hubeny, and D. L. Lambert, *Astrophys. J.* **591**, 1192 (2003).
42. C. Sneden, I. I. Ivans, and R. P. Kraft, *Mem. Soc. Astron. Ital.* **71**, 657 (2000).

43. E. A. Gurtovenko and R. I. Kostyk, *Fraunhofer Spectrum and System of Solar Oscillator Strengths* (Naukova Dumka, Kiev, 1989) [in Russian].
44. M. C. Gálvez-Ortiz, J. R. A. Clarke, D. J. Pinfield, J. S. Jenkins, S. L. Folkes, A. E. G. Pérez, A. C. Day-Jones, B. Burningham, H. R. A. Jones, J. R. Barnes, and R. S. Pokorny, *Mon. Not. R. Astron. Soc.* **409**, 552 (2010).
45. J. R. A. Clarke, D. J. Pinfield, M. C. Gálvez-Ortiz, J. S. Jenkins, B. Burningham, N. R. Deacon, H. R. A. Jones, R. S. Pokorny, J. R. Barnes, and A. C. Day-Jones, *Mon. Not. R. Astron. Soc.* **402**, 575 (2009).
46. J. R. A. Clarke, PhD Thesis (Univ. Hertfordshire, Hertfordshire, UK, 2011).
47. Ya. V. Pavlenko, H. R. A. Jones, Yu. Lyubchik, J. Tennyson, and D. J. Pinfield, *Astron. Astrophys.* **447**, 709 (2006).
48. M. K. Kuznetsov, Ya. V. Pavlenko, and M. K. Galvez-Ortiz, *Kinem. Phys. Celest. Bodies* **28**, 280 (2012).
49. J. Frith, D. J. Pinfield, H. R. A. Jones, J. R. Barnes, Y. Pavlenko, E. L. Martin, C. Brown, M. K. Kuznetsov, F. Marocco, R. Tata, and M. Cappetta, *Mon. Not. R. Astron. Soc.* **435**, 2161 (2013); arXiv:1308.0501v1 [astro-ph.GA] (2013).

*Translated by G. Rudnitskii*